HNPS Advances in Nuclear Physics

Vol 32 (2026)

HNPS2025

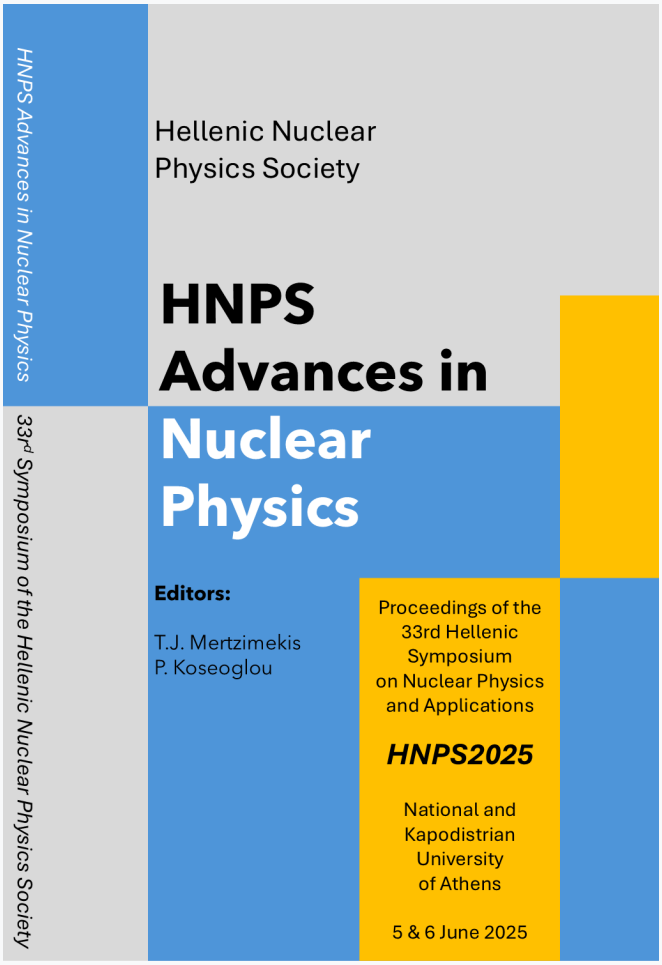


# Ground-state lifetime measurements in Tellurium decay chains: Analysis and Results

*Margarita Efstathiou, Pavlos Koseoglou, Polytimos Vasileiou, Theo J. Mertzimekis, Aikaterini Zyriliou, Angelos Karadimas, Constantin Mihai, Nicolae Marius Marginean, Razvan Lica, Cristian Costache, Andrei Turturica, Radu-Emanuel Mihai, Ruxandra Borcea, Raluca Marginean, Nicoleta Florea, Dennis Bonatsos, Andriana Martinou, Nikolay Minkov*

doi: 10.12681/hnpsanp.8678



**To cite this article:**

Efstathiou, M., Koseoglou, P., Vasileiou, P., Mertzimekis, T. J., Zyriliou, A., Karadimas, A., Mihai, C., Marginean, N. M., Lica, R., Costache, C., Turturica, A., Mihai, R.-E., Borcea, R., Marginean, R., Florea, N., Bonatsos, D., Martinou, A., & Minkov, N. (2026). Ground-state lifetime measurements in Tellurium decay chains: Analysis and Results. *HNPS Advances in Nuclear Physics*, *32*, 25–31. https://doi.org/10.12681/hnpsanp.8678

*HNPS Advances in Nuclear Physics* Vol. **32**, 25–31 (2025)
doi: 10.12681/hnpsanp.8678

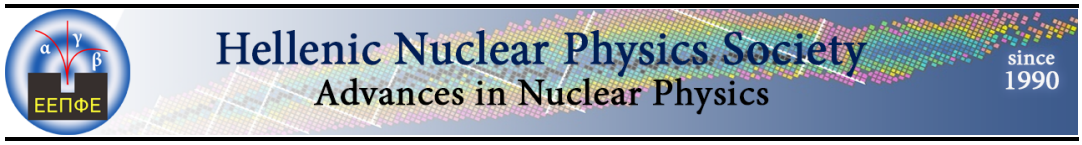


ARTICLE

# Ground-state lifetime measurements in Tellurium decay chains: Analysis and Results.

M. Efstathiou,[*,1] P. Koseoglou,[1,2] P. Vasileiou,[1] T.J. Mertzimekis,[1] A. Zyriliou,[1] A. Karadimas,[1] C. Mihai,[3] N. Margineăn,[3] R. Lică,[3] C. Costache,[3] A. Turturica,[3] R.E. Mihai,[3,4] R. Borcea,[3] R. Margineăn,[3] N. Florea,[3] D. Bonatsos,[5] A. Martinou,[5] and N. Minkov[6]

[1]Department of Physics, National and Kapodistrian University of Athens, Zografou Campus, GR-15784, Greece
[2]Technische Universität Darmstadt, Institute for Nuclear Physics, Schlossgartenstr. 9, 64289 Darmstadt, Germany
[3]Horia Hulubei National Institute of Physics and Nuclear Engineering - IFIN-HH, R-077125 Bucharest, Romania
[4]Institute of Experimental and Applied Physics, Czech Technical University in Prage, Huzova 240/5 11000, Prague 1, Czech Republic
[5]Institute of Nuclear and Particle Physics, NCSR Demokritos, GR-15310 Agia Paraskevi, Greece
[6]Institute of Nuclear Research and Nuclear Energy, Bulgarian Academy of Sciences, BG-1784 Sofia, Bulgaria
*Corresponding author: margefst@phys.uoa.gr

(Received: 20 Oct 2025; Accepted: 19 Nov 2025; Published: 20 Nov 2025)

**Abstract**
The isotopes of Tellurium are located near the stability line on the isotopic chart, making them important for study in the context of nuclear theory and in terms of applications. In this work, we present a study of the radioactive decay chains of Tellurium isotopes with mass numbers 117 and 115, aiming to investigate their ground-state half-lives as determined from an experiment conducted at the 9 MV Tandem accelerator at IFIN-HH in Romania. Key parts of this presentation are a novel approach used to extract the experimental half-life values, as well as its application to the experimental data obtained for the two Tellurium decay chains. A comparison of the results for the half-lives obtained with and without the application of this approach will also be presented to demonstrate its capabilities. The approach does not rely on any input from the literature, and it allows for a significant reduction in the uncertainties associated with the extracted half-life values, thus enhancing the reliability and precision of the results.

**Keywords:** activation; 2n-transfer reaction; lifetime

## 1. Introduction

The isotopes of Tellurium are located just above the closed nuclear shell at Z = 50, a fact that makes them ideal study cases of nuclear structure [1], as well as for investigating the interplay between collective and single-particle degrees of freedom and relevant phenomena, such as shape coexistence and shape evolution.

 ISBN 2654-007X (print), 2654-0088 (online).

Some Te (Tellurium), Sb (antimony) and Sn (tin) isotopes are significant in terms of applications since they are used in nuclear medicine. More specifically, some of their unstable isotopes are utilized both for diagnosing and treating cancer. For example, $^{117m}$Sn is particularly interesting because it emits conversion electrons and Auger electrons with a short range of action, offering targeted therapy, while also emitting gamma radiation for imaging [2].

It is also important to note that the existing literature half-live values of the ground states of the isotopes presented in this work were determined in experiments conducted many years ago and the error handling is not described clearly [3–5]. In the present work the half-lives ($t_{1/2}$) are re-examined and measured using modern facilities and contemporary detectors. Also, accurate half-life values of Sn, Sb and Te isotopes are important for nuclear-medicine applications, as they affect dosimetry and radionuclide availability, and although this work focuses on ground-state decays, the same considerations also apply to medically relevant isomeric states such as $^{117m}$Sn.

A analysis method is introduced to reduce the uncertainties associated with experimental errors in the activation method. This approach complements nuclear structure studies in the same mass region. As a result, lifetime uncertainties are improved, and new adopted values are proposed.

## 2. Experimental Details

The experiment was carried out at the 9 MV Tandem accelerator of IFIN-HH in Măgurele, Bucharest [6] (see Fig. 1a). A $^{nat}$Ag target with composition of 51.8% $^{107}$Ag and 48.2% of $^{109}$Ag was used. The target had a thickness of 5.24 mg/cm$^2$. The target was bombarded with $^{11}$B ions at an energy of 35 MeV to populate the states of $^{116,118}$Te via the $^{nat}$Ag($^{11}$B, $xn$)$^{116,118}$Te reaction. The intensity of the beam was 4-9 nA and the charge state of the beam was $q = 5^+$ [7].

**(a)** The 9 MV Tandem accelerator.

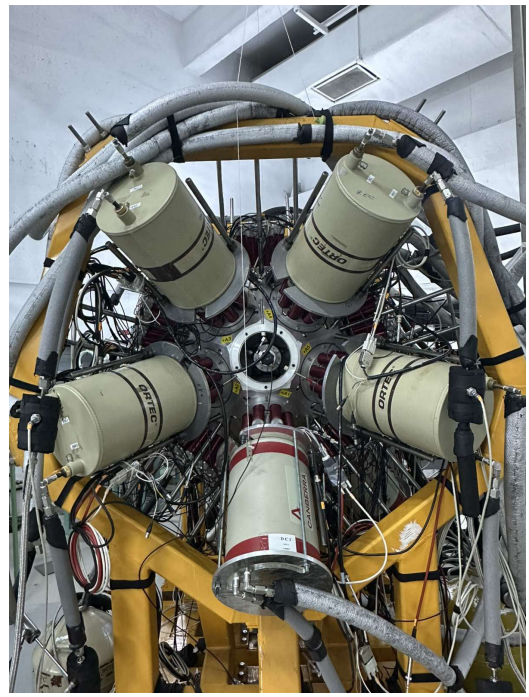


**(b)** The ROSPHERE array.

**Figure 1.** Experimental setup.

The ROSPHERE (ROmanian array for SPectroscopy in HEavy ion REactions) [8] is a detector setup for $\gamma$-ray spectroscopy. ROSPHERE can accommodate up to 25 detectors of two types: high-purity germanium (HPGe) semiconductor detectors and $LaBr_3$(Ce) scintillators. The array has a spherical geometry and is composed of five rings, each having five available positions for detectors. These five rings are positioned at specific angles of 37°, 70°, 90°, 110°, and 143° with respect to the beam axis (see Fig. 1b) [8]. The specialized array is designed for nuclear-structure studies, including angular correlation measurements and lifetime determinations of nuclear excited states. The present experimental setup enables the investigation of half-lives spanning several orders of magnitude through the selection of an appropriate detector configuration. In the current study, the activation method was employed.

In the experiment presented in this work, the HPGe detectors were placed in the 1st, 3rd, and 5th rings of the ROSPHERE array at angles of 37°, 90°, and 143°, respectively, while the 2nd and 4th rings were filled with $LaBr_3$(Ce) detectors positioned at 70° and 110°, respectively, for fast-timing measurements.

The total irradiation time of the natural Ag target was approximately 199 h (≈8.3 d), followed by a total counting time of 26 h. The data were collected in 39 individual *runs*, each corresponding to a single HPGe $\gamma$-ray spectrum. The first six runs were acquired for 15 min each in order to properly sample the decay of the short-lived isotope $^{115}$Sb [9]. This corresponds to a total measuring time of about 90 min, i.e. roughly three half-lives of $^{115}$Sb ($t_{1/2}$ = 32 min). The transition from 15-min to 45-min runs was performed continuously, without any interruption in the data-acquisition sequence. Subsequently, 33 runs were recorded with a duration of 45 min each. Only data from the HPGe detectors were used in the present analysis, since they provide superior energy resolution compared to the $LaBr_3$ detectors, which were therefore excluded from the half-life evaluation. Event sorting and single-spectrum extraction were performed using the GASPware analysis package [10]. Also a standard $^{152}$Eu point source was employed for the energy and efficiency calibration of the detection system.

## 3. The Analysis

The analysis of these experimental data is based on the standard activation method, in which the decay curve of the studied $\gamma$-ray is constructed by plotting the measured counts of the $\gamma$-ray as a function of time. Each experimental point corresponds to a single run. The counts were measured for all the runs until the studied $\gamma$-ray vanished.

To analyse the data, a new approach was used. The aim of this analytical approach, which was used in this study, is first to correct the position of the experimental points on the time axis of the decay curve and to minimize the error. As mentioned before, 39 spectra were measured. For each spectrum, the counts per second for the peak of interest were calculated. The question is where each experimental point should be placed on the time axis. In order to explain the approach, Fig. 2 is used.

The initial time collection is to place each data point at the midpoint of its measurement interval ($t'$). In this case, the uncertainty is taken as half of the run duration, which results in a significant error. Using this approach, the decay constant $\lambda'$ is initially estimated by fitting the decay curve using the midpoint-assigned data. However, aside from the large errors in this case, the approach does not assign the correct time point to each measurement, because in this approach, the counts are split equally on both sides of the time. However, it is known that radioactive decay is not constant, but decreases over time. Therefore, the most appropriate time assigned of its data point is the one at which half of the de-excitations have occurred.

To determine, in each case, the desired time at which half of the de-excitations have taken place, it

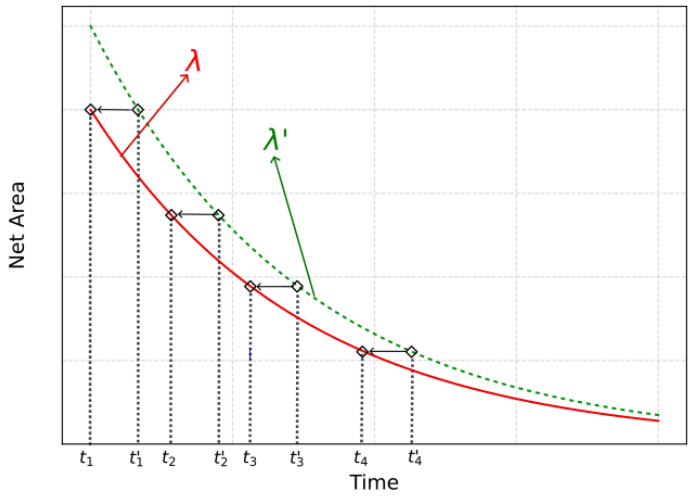


**Figure 2.** The theoretical representation of the shift of the points over time. The diagram illustrates how the points –and consequently the decay curve– have been shifted through the use of the approach.

is sufficient to solve the following integral:

$$\int_{t_i}^{t} N(t'')\,dt'' = \int_{t}^{t_{i+1}} N(t'')\,dt'' \tag{1}$$

In the current formula, $N(t'')$ is the function that represents the number of de-excitations occurring, $t$ is the time being evaluated (the time at which half of the decays occurred), and $t_i$ and $t_{i+1}$ are respectively the start and end of the measurement for the respective run. Solving this equation yields:

$$t = \frac{-1}{\lambda'} \cdot \ln\left(\frac{e^{-\lambda' t_{i+1}} + e^{-\lambda' t_i}}{2}\right) \tag{2}$$

By using this formula in Eq. (2), time uncertainties are refined via error propagation that includes $\lambda$, $t_i$, and $t_{i+1}$. As seen in Fig. 2, the corrected time points yield a slightly left-shifted decay curve and a more accurate half-life value. To better understand the above process, the case with $t_{1/2} = 45$ minutes and $\Delta t = 20$ (duration time of the runs) minutes is shown in Fig. 3 as a theoretical example.

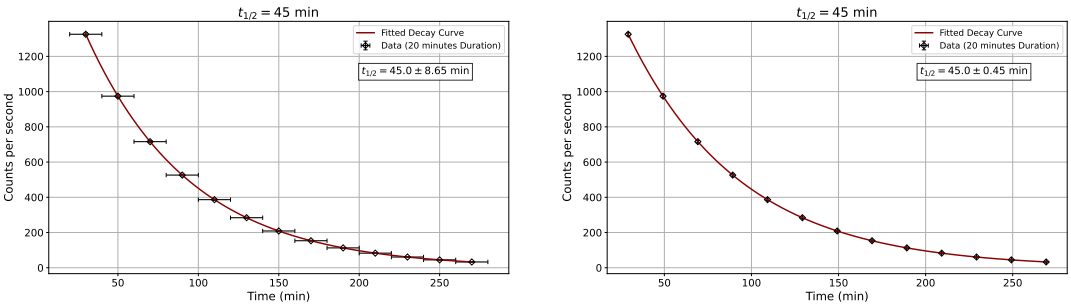


**(a)** Before applying Eq. (2)

**(b)** After applying Eq. (2)

**Figure 3.** Comparison before and after applying Eq. (2)

To verify whether this approach functions correctly, some theoretical calculations have been performed to estimate approximately how much the points shift in each case and how much the error

is reduced by this correction. The cases studied involve different choices of measurement durations and various selections of half-lives.

This analysis was performed for three half-life values: 20, 45, and 180 minutes. For each of these half-life values, the analysis was conducted for six different $\Delta t$ values in the case where the half-life was 20 minutes, and for nine different $\Delta t$ values in the cases where the half-life was 45 and 180 minutes. It is important to mention that in each case, the de-excitation is monitored until it is nearly complete, which corresponds to approximately six times the $t_{1/2}$ being examined.

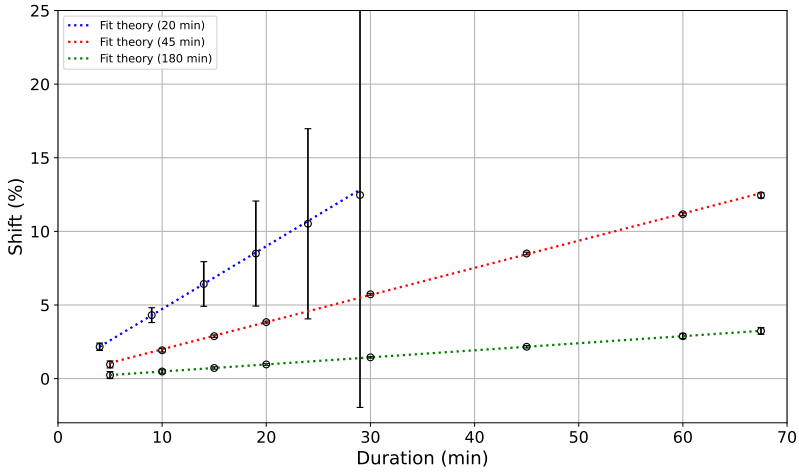


**Figure 4.** It shows the percentage by which the points are shifted to shorter times when the approach is applied to the scenarios under study. A slight horizontal offset is applied to the x-axis values for the 20-minute half-life data to prevent the large uncertainty of the last point from overlapping with the points of the other two series.

As shown in Fig. 4, the percentage shift varies depending on the half-life being studied and the chosen measurement duration. The term percentage shift refers to the percentage by which the points were shifted to the left along the x-axis after the application of the approach used in the present study. It is observed that shorter measurement durations result in smaller shifts, meaning that, in the limit of a 1-second measurement duration, the decay curve produced by the activation method would be essentially accurate and would not require any correction for half-lives significantly longer than 1 second, as is the case in the examples presented. Furthermore, the correction is more critical for short half-lives and becomes less significant for longer ones. However, as is evident in Fig. 4 and as mentioned above, the measurement duration plays an even more important role.

Fig. 5 clearly illustrates the importance of the correction in reducing the uncertainty of the fitted half-lives. In contrast to a simple dependence on the half-life itself, the relative error is strongly affected by the ratio between the measurement duration and the half-life. As the duration of each run approaches or exceeds the half-life of the isotope, the relative uncertainty increases rapidly, making the correction particularly relevant under such conditions. Furthermore, the graph provides a useful guide for selecting appropriate measurement intervals for a given decay constant. The substantial reduction in relative error after applying the correction highlights its significance and justifies its implementation in the analysis.

## 4. Results and Discussion

The approach described in the previous sections was used to measure the half-lives of the ground states of $^{117}$Sb, $^{117}$Sn, and $^{115}$Sn. It is important to note that it was not possible to measure the ground

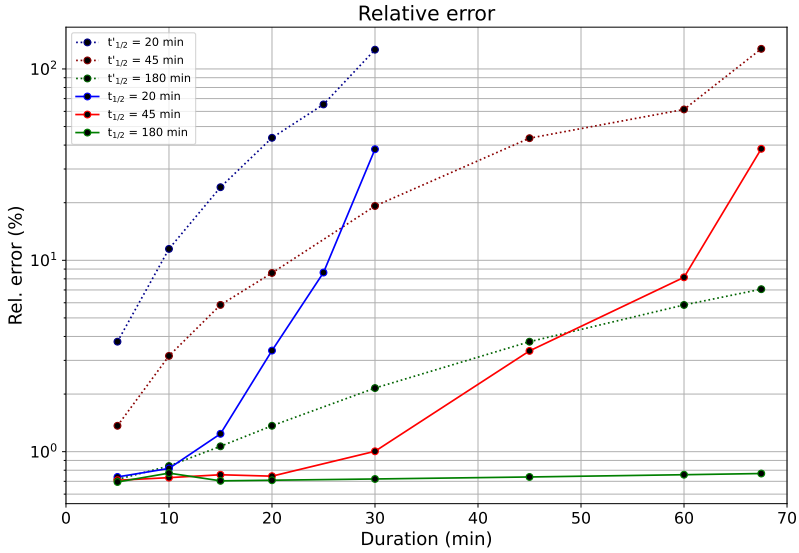


**Figure 5.** The plot shows the relative error in the adjusted half-life, for the values discussed earlier, both before and after the correction. The y-axis is logarithmic.

state of $^{115}$Sb due to the short half-life of this level. This state decays with a half-life of either 6.7 minutes or 5.8 minutes [9], which means that any gamma rays emitted from its de-excitation had already vanished within the first two runs. The results for the half-lives of the ground states of $^{117}$Sb, $^{117}$Sn, and $^{115}$Sn are shown in Table 1.

**Table 1.** The table presents the isotope under study, measured energy level, and comparison of the half-life values: before applying the present approach, after applying it, and the corresponding NuDat literature value [9].

| Isotope g.s | $E_{lvl}$ (keV) | $t_{1/2}$ Before (min) | $t_{1/2}$ After (min) | NNDC (min) |
|---|---|---|---|---|
| $^{117}$Te g.s. | 719.7(7) | 66.4(41) | 65.5(13) | 62(2) |
| $^{117}$Sb g.s. | 158.6(15) | 171.5(47) | 170.1(22) | 168.0(6) |
| $^{115}$Sb g.s. | 497.3(8) | 32.0(44) | 31.3(7) | 32.1(3) |

The approach significantly reduces errors, thus improving the accuracy of half-life measurements. As shown in Table 1, the results after using the approach exhibit greater accuracy compared to those in which the approach has not been applied. Also, as shown in Table 1, the results demonstrate clear improvements in certain cases compared to the existing literature values. Specifically, the measurement of $^{117}$Te shows higher precision compared to previously published data. Furthermore, as seen in the other two cases involving the isotopes $^{117}$Sb and $^{115}$Sb, the measured values are in agreement with the literature values. Overall, the approach has proven effective and is intended for use in future measurements.

This new approach can be applied to experiments carried out at modern research facilities, such as IFIN-HH, where a high-resolution gamma detector array was used. Additionally, revising the values found in the literature is considered necessary, given the age of the original measurements and the limitations of the experimental setups of that time. Finally, from an application perspective, the mass region of Sn, Sb, and Te has proven particularly important for the field of medical physics, as several unstable isotopes are either used as radiopharmaceuticals [11] or participate in their production, and

precise knowledge of their half-lives is essential for such nuclear medicine applications.

## Acknowledgements



**Acknowledgments**

PK was funded by the Deutsche Forschungsgemeinschaft (DFG, German Research Foundation) – 539757749.

This project has received funding from the European Union's Horizon Europe Research and Innovation programme under Grant Agreement No 101057511 (EURO-LABS).

All the authors are grateful to the ROSPHERE and SORCERER collaborations for providing the equipment used for the measurements presented in this work.

## References

[1] T. D. Morris, J. Simonis, S. R. Stroberg, C. Stumpf, G. Hagen, J. D. Holt, G. R. Jansen, T. Papenbrock, R. Roth, and A. Schwenk. "Structure of the Lightest Tin Isotopes". In: *Phys. Rev. Lett.* 120 (15 2018), p. 152503. DOI: 10.1103/PhysRevLett.120.152503.

[2] C. Apgar. *Production of $^{117m}$Sn and $^{119m}$Te via Proton Bombardment on Natural Antimony: Applications for Charged Particle Reaction Modeling and Theranostics*. University of California, Berkeley, 2024. URL: https://www.proquest.com/dissertations-theses/production-sup-117m-sn-119m-te-via-proton/docview/3110986222/se-2.

[3] G. Berzins, W.H. Kelly, G. Graeffe, and W.B. Walters. "Ge(Li) and NaI(Tl) studies of the decay of $^{117}$Te". In: *Nuclear Physics A* 104.2 (1967), pp. 241–262. DOI: 10.1016/0375-9474(67)90553-2.

[4] R. W. Fink, G. Andersson, and J. Kantele. "Nuclear Spectroscopy of Mass-Separated Neutron-Deficient Tellurium Isotopes." In: *Arkiv Fysik* Vol: 19 (Dec. 1960). URL: https://www.osti.gov/biblio/4016367.

[5] E. Hagebø. "Yields and isomeric yield ratios of antimony isotopes from the interaction of 159 MeV to 18· 2 GeV protons with uranium". In: *Journal of Inorganic and Nuclear Chemistry* 29.10 (1967), pp. 2515–2532. DOI: 10.1016/0022-1902(67)80177-5.

[6] IFIN-HH. *9 MV FN Pelletron Tandem Accelerator, https://tandem.nipne.ro/9MV_Pelletron.php*.

[7] A. Zyriliou et al. *Exploring collectivity and shape coexistence in neutron-deficient Te nuclei*. Tech. rep. Department of Physics, University of Athens, Greece, 2022.

[8] D. Bucurescu et al. "The ROSPHERE $\gamma$-ray spectroscopy array". In: *Nuclear Instruments and Methods in Physics Research Section A: Accelerators, Spectrometers, Detectors and Associated Equipment* 837 (2016), pp. 1–10. ISSN: 0168-9002. DOI: 10.1016/j.nima.2016.08.052.

[9] NNDC. *National Nuclear Data Center, http://www.nndc.bnl.gov/*.

[10] N. Mărginean, C. A. Ur, and D. Bazzacco. *The GASPware data analysis package for nuclear spectroscopy*. GitHub: https://github.com/sztaylor89/GASPware-1.git. 1991.

[11] S. C. Srivastava. "A Bridge not too Far: Personalized Medicine with the use of Theragnostic Radiopharmaceuticals". In: *J. Postgrad. Med. Educ. Res.* 47 (2013), pp. 31–46.